

DMD #41046

## Title Page

# **Role of residue 87 in the activity and regioselectivity of clozapine metabolism by drug metabolizing CYP102A1 M11H: application for structural characterization of clozapine GSH conjugates**

Vanina Rea, Sanja Dragovic, Jan Simon Boerma, Frans J.J. de Kanter, Nico P.E. Vermeulen and Jan N.M. Commandeur

Division of Molecular Toxicology, LACDR, Leiden/Amsterdam Center for Drug Research, Faculty of Sciences, Vrije Universiteit, De Boelelaan 1083, 1081 HV Amsterdam, The Netherlands. VR, SD, JSB, NPEV, JNMC

Division of Organic and Inorganic Chemistry, Faculty of Sciences, Vrije Universiteit, De Boelelaan 1083, 1081 HV Amsterdam, The Netherlands. FFJDK

DMD #41046

**Running title:** Regioselective metabolism of clozapine by CYP102A1-mutants.

**Corresponding author:**

J.N.M. Commandeur, Division of Molecular Toxicology, LACDR, Leiden/Amsterdam Center for Drug Research, Faculty of Sciences, Vrije Universiteit, De Boelelaan 1083, 1081 HV Amsterdam, The Netherlands; e-mail address: j.n.m.commandeur@vu.nl.

**Document statistics:**

Number of pages: 27

Number of tables: 2

Number of figures: 5

References: 27

Abstract: 222 words

Introduction: 1078 words

Discussion: 1639 words

**Abbreviations**

CDNB, 1-chloro-2,4-dinitrobenzene; CYP102A1 M11H, cytochrome P450 102A1 mutant M11 His-tagged (Damsten et al., 2008); hGST P1-1, human glutathione S-transferase P1-1.

## Abstract

In the present study, a site-saturation mutagenesis library of drug metabolizing CYP102A1 M11H with all 20 amino acids at position 87 was applied as biocatalyst for the production of stable and reactive metabolites of clozapine. Clozapine is an atypical antipsychotic drug where formation of reactive metabolites is considered to be responsible for several adverse drug reactions. Reactive intermediates of clozapine can be inactivated by GSH to multiple GSH conjugates, by non-enzymatic and glutathione S-transferase (GST) mediated conjugation reactions. The structures of several GST dependent metabolites have not yet been elucidated unequivocally. The present study shows that the nature of amino acid at position 87 of CYP102A1 M11H strongly determines both activity and regioselectivity of clozapine metabolism. Some mutants showed preference for N-demethylation and N-oxidation, whereas others showed high selectivity for bioactivation to reactive intermediates. The mutant containing Phe87 showed both high activity and high selectivity for the bioactivation pathway and was used for the large scale production of GST dependent GSH conjugates by incubation in presence of recombinant human glutathione S-transferase P1-1. Five human relevant GSH adducts were produced at high levels enabling structural characterization by <sup>1</sup>H-NMR. This work shows that drug metabolizing CYP102A1-mutants, in combination with GSTs, are very useful tools for the generation of GSH conjugates of reactive metabolites of drugs in order to enable their isolation and structural elucidation.

## Introduction

Cytochrome P450 (P450s) are involved in the metabolism of approximately 80% of the drugs currently on the market (Shimada et al., 1994; Evans et al., 1999). In some cases drugs can be oxidized by P450s to electrophilic reactive intermediates, which subsequently can react with nucleophilic functional groups in biomolecules such as proteins and DNA. Also, stable metabolites might possess pharmacological activities that might be responsible for undesired adverse drug reactions. It is for these reasons that also the characterization of the biological properties of major metabolites is considered to be important for drug safety assessment (Smith and Obach, 2009). Therefore, methods are required to obtain the relevant drug metabolites in sufficient yield to allow structural elucidation and to study their pharmacological and toxicological properties. Metabolite production can be achieved by organic synthesis, electrochemical oxidation of parent drug and by biosynthesis using specific P450s. In particular, mutants of the bacterial cytochrome P450 CYP102A1 (P450 BM3) are considered to have good perspective for the large scale production of human relevant drug metabolites, as this very stable enzyme possesses the highest activity ever recorded for a P450 (Ost et al, 2000). By combinations of site-directed and random mutagenesis many CYP102A1 mutants have been obtained which are able to convert drugs and drug-like molecules to human relevant metabolites (Van Vugt-Lussenburg et al., 2007; Yun et al., 2007; Sawayama et al., 2009; Kim et al., 2011). In our previous work, four mutants of CYP102A1 have been evaluated as biocatalysts for the bioactivation of several drugs to reactive intermediates (Damsten et al., 2008). Drugs tested were acetaminophen, diclofenac and clozapine (CLZ), and formation of reactive intermediates was analyzed by measurement of GSH conjugates. For all drugs tested, most stable metabolites and reactive intermediates were produced at much higher activity by the CYP102A1-mutants than by human and rat liver microsomes, supporting their potential for use in characterization of toxicologically relevant metabolites (Damsten et al., 2008).

Recently, the highly active drug-metabolizing mutant CYP102A1 M11H was used to investigate the role of human glutathione S-transferases in the inactivation of CLZ (Dragovic et al., 2010). CLZ is an atypical antipsychotic drug showing a low incidence of extrapyramidal side effects combined with excellent antipsychotic efficacy in schizophrenic and manic treatment-resistant patients (Buchanan, 1995; Safferman et al., 1991; Wagstaff and Perry, 2003). Approximately 1-2 % of patients develop agranulocytosis. Enhanced serum

## DMD #41046

transaminases were monitored with 37% of the patients while 0.06% of the patients had liver failure (Hummer et al., 1997). It is still unknown which factors predispose part of the patient population to these forms of CLZ toxicity. Based on the identification of several GSH conjugates, formation of a reactive nitrenium ion by peroxidases, hypochlorite and P450s has been proposed as a possible explanation for these ADRs (Fischer et al., 1991; Liu et al., 1995; Maggs et al., 1995; Pirmohamed et al., 1995). *In vitro* and *in vivo* studies of CLZ have shown the formation of four GSH-conjugates with identical mass with  $MH^+$  ion at  $m/z$  632.2 and one deschlorinated GSH conjugate with  $MH^+$  ion at  $m/z$  598.3. All conjugates can be explained by direct conjugation of GSH at different positions of a reactive nitrenium ion and by chloro-substitution of the nitrenium ion followed by reduction, see Figure 1 (Maggs et al., 1995; Dragovic et al, 2010). Unequivocal structure determination by  $^1H$ -NMR has been published for only two of the glutathione conjugates of CLZ (Fischer et al., 1991; Liu et al., 1995; Madsen et al., 2007). The major GSH conjugate (CG-1, Figure1) was found to be conjugated at position 6 of the chlorinated aromatic ring, whereas a minor GSH conjugate (CG-3, Figure 1) was found to be conjugated at position 9 (Fischer et al., 1991; Liu et al., 1995). A third GSH conjugate with a  $MH^+$  ion at  $m/z$  632.2 was only identified in *in vitro* incubations with human and rat liver microsomes and was tentatively assigned to position 7 (CG-4, Figure 1). Two GSH-conjugates, with  $MH^+$  ion at  $m/z$  632.2 and 598.3, were first discovered in bile of treated mice and rats and were originally proposed to originate from unidentified reactive intermediates formed *in vivo* (Maggs et al., 1995). However, we recently demonstrated that these GSH conjugates, CG-5 and CG-6 in Figure 1, are formed at high levels when CLZ incubations with purified CYP102A1 M11H and human liver microsomes were supplemented with human glutathione S-transferases (Dragovic et al., 2010). Three of the four tested human glutathione S-transferases (hGSTs) showed strongly increased total GSH conjugation and also resulted in formation of different regioisomeric GSH conjugates of CLZ, Figure 1 (Dragovic et al., 2010).

For two of the GSH conjugates that have been found previously, the structure has not been elucidated by NMR. Conjugate CG-4, which was found in incubations of CLZ with human liver microsomes, was tentatively assigned as conjugate at position 7 (Maggs et al., 1995). GSH conjugate CG-5, which was identified in bile of rats and mice, was proposed to result from GSH conjugation to the non-chlorinated ring (Maggs et al., 1995). The aim of the present study was to identify the structures of these GSH conjugates by  $^1H$ -NMR, by performing large scale incubations of CLZ with selective CYP102A1 M11H-mutants in presence of glutathione S-transferase. Because GST P1-1 appeared to be the most active hGST

## DMD #41046

in the formation of enzyme-dependent GSH conjugates (Dragovic et al., 2010), this enzyme was selected for large scale production of GSH conjugates.

Although CYP102A1 M11H was previously shown to produce high levels of CLZ metabolites, the most abundant metabolites appeared to be N-demethylclozapine and CLZ N-oxide (Damsten et al., 2008; Dragovic et al., 2010). As a consequence, also GSH conjugates derived from these metabolites were produced, which strongly complicates isolation of CG-4 and CG-5. Recently, we showed that by changing the active site residue at position 87 of CYP102A1 M11H the regioselectivity of testosterone hydroxylation was strongly modified (Vottero et al., 2011). Therefore, in the present study, we first evaluated the effect of mutation at position 87 on the regioselectivity of CLZ metabolism in order to identify the most suitable biocatalyst for the bioactivation of CLZ and subsequent structural characterization of the formed GSH conjugates. The results show that the nature of the residue at position 87 strongly influences regioselectivity of CLZ metabolism and that by using a more selective P450 CYP102A1 M11H-mutant all five human relevant GSH conjugates of CLZ could be produced in high levels, enabling structural elucidation by  $^1\text{H-NMR}$ .

## Materials and methods

### Materials

All chemicals were of analytical grade and obtained from standard suppliers.

### Library construction

Site directed mutants of CYP102A1 M11H at position 87 were constructed by mutagenic PCR using the Stratagene QuikChange XL site-directed mutagenesis kit (Stratagene, La Jolla, CA, USA) using 20 complementary pairs of mutagenesis primers (Vottero et al., 2011). The mutagenic PCR was applied to a pBluescript vector containing the gene of the drug metabolizing CYP102A1 M11H, flanked by EcoR1 and BamH1 restriction sites. CYP102A1 M11H contains mutations R47L, E64G, F81I, F87V, E143G, L188Q, Y198C, E267V, H285Y and G415S when compared to wild-type CYP102A1 (Damsten et al., 2008). The sequence of the forward primers were as follows: 5'-GCA GGA GAC GGG TTA **XXX** ACT AGT TGG ACG CAT-3'. The **XXX** represents the codon that was used to introduce the specific mutation at position 87. The reverse primer for the mutagenic PCR was a 34-mer 5'-CAT GCG TCC AAC TAG TYY YTA ACC CGT CTC CTG C-3' in which the **YYY** is the reverse complement of codon **XXX**. The underlined bases indicate a new SpeI digestion site. The following codons (**XXX**) were used: Ala, GCC; Arg, CGG; Asn, AAC; Asp, GAC; Cys, UGC; Gln, CAG; Glu, GAG; Gly, GGG; His, CAC; Ile, AUC; Leu, CUG, Lys, AAG; Met, AUG; Phe, UUC; Pro, CCC, Ser, UCC; Thr, ACC; Trp, UGG; Tyr, UAC, and Val, GUG. After mutagenic PCR, the plasmids were digested with EcoR1 and BamH1 restriction enzymes and the genes of mutated CYP102A1 M11H were cloned into a pET28a+ vector, which encodes for a N-terminal His-tag. The desired mutations in the P450 domain were confirmed by DNA sequencing (Baseclear, Leiden, The Netherlands).

### Expression, isolation and purification of enzymes

Expression of the P450 CYP102A1 M11H-mutants was performed by transforming competent *E. Coli* BL21 cells with the pET28+-vectors, as described previously (Vottero et al., 2011). Proteins were purified using Ni-NTA agarose, after which P450 concentrations were determined using carbon monoxide (CO) difference spectrum assay. Purity of the enzymes was checked by SDS PAGE electrophoresis on 12% gel and Coomassie-staining. Protein purity was higher than 98% in all samples obtained.

## DMD #41046

Human GST P1-1 was prepared and purified as described previously (Dragovic et al., 2010). Protein concentration was determined according to the method of Bradford (Bradford et al., 1976) with reagent obtained from Bio-Rad. The specific activity of the purified GST was assayed according to Habig et al. (Habig et al., 1974). The specific activity of the purified recombinant human GST P1-1 using CDNB as a substrate was 27.9  $\mu\text{mol}/\text{min}/\text{mg}$  protein.

### **Metabolism of CLZ by CYP102A1 M11H-mutants in presence of human GST P1-1**

Incubations using CYP102A1 M11H-mutants as bioactivation system were performed at a final enzyme concentration of 250 nM, as described previously (Damsten et al., 2008). All incubations were performed in 100 mM potassium phosphate buffer (pH 7.4) and at a final volume of 250  $\mu\text{L}$ . The substrate CLZ was incubated at a concentration of 500  $\mu\text{M}$ . GST P1-1 in concentration of 8  $\mu\text{M}$  and 100  $\mu\text{M}$  GSH were added to the incubations in order to trap reactive CLZ nitrenium ion. Reactions were initiated by the addition of a NADPH regenerating system (0.2 mM NADPH, 1 mM glucose-6-phosphate, 0.4 U/mL glucose-6-phosphate dehydrogenase, final concentrations) and performed for 30 min at room temperature. In this time period, product formation was linear, as described previously (Damsten et al., 2008). Reactions were terminated by addition of 25  $\mu\text{L}$  10%  $\text{HClO}_4$ , and centrifuged for 15 min at 14000 rpm. The supernatants were analyzed by reversed-phase liquid chromatography using a Luna 5  $\mu\text{m}$  C18 column (150 mm  $\times$  4.6 mm i.d.) from Phenomenex as stationary phase, protected by a 4.0 mm  $\times$  3.0 mm i.d. security guard (5  $\mu\text{m}$ ) C18 guard column (Phenomenex, Torrance, CA, USA). The gradient used was constructed by mixing the following mobile phases: eluent A (0.8 % acetonitrile, 99 % water, and 0.2 % formic acid); eluent B (99 % acetonitrile, 0.8 % water, and 0.2 % formic acid). The first 5 min were isocratic at 0 % eluent B; from 5 to 30 min the percentage of eluent B linearly increases to 100 %; from 30 to 35 min linear decrease to 0 % B and maintained at 0 % for re-equilibration until 40 min. The flow rate was 0.5 mL/min.

Samples were analyzed using LC-MS/MS for identification and using UV/VIS detection at 254 nm for quantification. The Shimadzu Class VP 4.3 software package was used for determination of peak areas in the UV chromatograms. A standard curve of CLZ was used to estimate the concentrations of the metabolites, assuming that the extinction coefficients of the metabolites at 254 nm are equal to that of CLZ. UV-VIS-spectra of clozapine and its



## DMD #41046

metabolites, as determined on line by diode array detection (180-400 nm), all showed similar spectra with maxima at 240, 260 and 295 nm (data not shown). The standard curve of CLZ was linear between 1 and 100  $\mu\text{M}$ ; the limit of quantitative detection by UV/VIS was estimated to be 0.1  $\mu\text{M}$  (data not shown).

For identification of the metabolites, an Agilent 1200 Series Rapid resolution LC system was connected to a hybrid quadrupole-time-of-flight (Q-TOF) Agilent 6520 mass spectrometer (Agilent Technologies, Waldbronn, Germany), equipped with electrospray ionization (ESI) source and operating in the positive mode. The MS ion source parameters were set with a capillary voltage at 3500 V; nitrogen was used as the desolvation and nebulizing gas at a constant gas temperature of 350 °C, drying gas 8 L/min and nebulizer 40 psig. Nitrogen was used as a collision gas with collision energy of 25V. MS spectra were acquired in full scan analysis over an  $m/z$  range of 50–1000 using a scan rate of 1.003 spectra/s. The MassHunter Workstation Software (version B.02.00) was used for system operation and data collection. Data analysis was performed using Agilent MassHunter Qualitative analysis software.

### **Large scale incubation**

The CLZ GSH conjugates produced on a preparative scale by large scale incubation with the most selective CYP102A1 M11H-mutant as biocatalyst. A 5 mL reaction volume containing 1  $\mu\text{M}$  purified enzyme, 500  $\mu\text{M}$  CLZ, 100  $\mu\text{M}$  GSH, 8  $\mu\text{M}$  GST P1-1, and an NADPH regenerating system (0.2 mM NADPH, 1 mM glucose-6-phosphate, 0.4 U/mL glucose-6-phosphate dehydrogenase) was prepared in 100 mM potassium phosphate buffer pH 7.4. The reaction was allowed to continue for 6h at 25°C. To achieve maximal conversion of CLZ, the incubation was supplemented every hour with 40  $\mu\text{L}$  of 120  $\mu\text{M}$  M11 Phe87, 20  $\mu\text{L}$  25 mM GSH, 500  $\mu\text{L}$  NADPH regenerating system and 100  $\mu\text{L}$  200  $\mu\text{M}$  GST P1-1. The final incubation volume was 8.4 mL. The reaction was terminated by adding 0.84 mL of 10 %  $\text{HClO}_4$  and centrifuged for 15 min at 14000 rpm. The supernatant was applied to a Strata X C-18 SPE column 200mg/3mL (Phenomenex, Torrance, CA, USA). The column was washed with 5 ml of  $\text{H}_2\text{O}$  to remove salts and proteins. CLZ and its metabolites were subsequently eluted using 2 mL of methanol. Sample was evaporated to dryness and reconstituted in 2 mL of eluent A (0.8% acetonitrile, 99% water, and 0.2% formic acid). The sample was applied by manual injection on a preparative chromatography column Luna 5  $\mu\text{m}$  C18(2) column (250

## DMD #41046

mm x 100 mm i.d.) from Phenomenex (Torrance, CA, USA) which was previously equilibrated with 100% eluent A. Flow rate of 2 mL/min and a gradient using the eluent A (0.8% acetonitrile, 99% water, and 0.2% formic acid) and B (99% acetonitrile, 1% water, and 0.2% formic acid) was applied for separation of formed CLZ metabolites. The first 10 min were isocratic at 0% eluent B; from 10 to 65 min, the percentage of eluent B increased linearly to 65%; from 65 to 70 min further increase of eluent B to 100%; from 70 to 80 min, there was a linear decrease to 0% B, and re-equilibration was maintained until 120 min. Metabolites were detected using UV detection (254 nm) and collected manually. Collected fractions were first analyzed for purity and identity by the analytical HPLC and LC-MS/MS methods as described above. The samples were evaporated to dryness under nitrogen stream and dissolved in 1 mL deuterium oxide to exchange acidic hydrogen atoms by deuterium atoms. Samples were evaporated to dryness in the vacuum concentrator, the residues were redissolved in 500  $\mu$ L of methyl alcohol- $d_4$  and  $^1\text{H-NMR}$  spectra were recorded at room temperature.  $^1\text{H-NMR}$ -analysis was performed on Bruker Avance 500 (Fallanden, Switzerland), equipped with cryoprobe.  $^1\text{H-NMR}$  measurements were carried out at 500.23 MHz.

## Results

### Expression of CYP102A1 M11H-mutants

A saturation mutagenesis library with a different residue at position 87 of CYP102A1 M11H was recently created in our lab (Vottero et al., 2011). All 20 mutants were expressed in *E. Coli* BL21 with pET28+-vectors; the P450 quantification was done by CO-difference spectrum. For the mutants Pro87, Asp87 and Ser87, the reduced CO difference spectra only showed a peak at 420 nm, suggesting that these amino acids negatively affect the folding and/or stability of CYP102A1 M11H. The mutant containing Asn87 showed a significant peak at 420 nm with intensity of almost equal to that at 450 nm. Mutants containing Met87, His87 and Gly87 showed a small shoulder at 420 nm next to the peak at 450 nm. All other mutants only produced peaks with maxima ranging from 448 nm to 450 nm (Vottero et al., 2011).

### Activity and regioselectivity of metabolism of CLZ by CYP102A1 M11H-mutants

When CLZ was incubated at analytical scale with the 20 different CYP102A1 M11H-mutants in presence of GSH and hGST P1-1 in total 13 different metabolites were found, Table 1, consistent with our previous studies (Damsten et al., 2008; Dragovic et al., 2011). Five of the metabolites result from N-oxidation (C-1), N-demethylation (C-2) and piperazine ring cleavage (C-3), and combinations of these (C-4 and C-5), Figure 1. In total eight different GSH conjugates were found resulting from bioactivation of CLZ to reactive intermediates. Five of these GSH conjugates result from addition reactions of the CLZ nitrenium ion with glutathione (CG-1, CG-3, CG-4, CG-5) and chlorine-substitution (CG-6). The LC-MS/MS spectra of these five GSH-conjugates are tabulated in Table 2; the assignment of the fragments have been described elsewhere (Maggs et al., 1995; Damsten et al., 2008; Dragovic et al., 2011). GSH conjugates designated CG-2 and CG-8 were found to be secondary GSH conjugates, resulting from bioactivation of N-demethylclozapine to its corresponding nitrenium ion and subsequent addition (CG-2) and chlorine-substitution (CG-8). CG-7 corresponds to a di-GSH conjugate that most likely results from GSH conjugation to the GSH containing nitrenium ion formed after chlorine substitution of the CLZ nitrenium ion, Figure 1.

As shown in Table 1, the nature of amino acid residue at position 87 has strong influence on both the activity and regioselectivity of formation of CLZ metabolites. As

## DMD #41046

indicated in the last column, generally highest activity was observed with mutants containing apolar amino acids at position 87. The mutants containing Ala87, Val87 and Ile87 showed the highest activity, followed by Phe87 and Trp87. Mutants containing Leu87, Met87, Gly87 and Pro87 showed only very low activity (<6% conversion). Among the mutants containing polar uncharged residues Tyr87 and Gln87 were the most active, showing 25.7% and 9.4% conversion, respectively. The mutants containing negative charged residue Asp87 and Glu87 had low activity with 7.4% and 2.4% conversion, respectively. For the mutant Asp87 no total activity could be calculated, as the P450 concentration could not be measured. The mutants containing positive charged residue His87, Arg87 were poorly active in the metabolism of CLZ (<2% conversion). The mutants having Lys87, Ser87, and Thr87 at position 87 did not show any activity.

Figure 2 shows the effect of amino acid residue 87 on the relative amounts of the stable metabolites formed via pathways a, b and c (Figure 1) and the relative amounts of GSH conjugates resulting from bioactivation of CLZ (pathway d, Figure 1). For all the mutants the major stable metabolite was N-demethylclozapine (C-2) followed by CLZ N-oxide (C-1), Figure 2A. Significant differences were observed in the ratios of C-2 to C-1. In case of mutants containing Ile87, Leu87, Met87 and Glu87, N-demethylation was up to ten-fold more abundant than N-oxidation. In contrast, mutants containing Phe87, His87, Asp87, Gly87 and Gln87 the ratio of N-demethylation to N-oxidation ranged from 1.2 to 2. The other stable metabolites (C-3, C-4 and C-5) represented only minor metabolites for all the mutants.

As illustrated in Figure 2B, the metabolic profile of the formed GSH adducts appears to be relatively constant for all the active mutants, supporting the hypothesis that all GSH conjugates originate from the CLZ nitrenium ion (Dragovic et al., 2010). In all cases, GSH conjugate CG-6 is the major metabolite and accounts for on average  $41 \pm 5\%$  of the total GSH conjugates. Considering the fact that conjugate CG-7 most likely also originates from the same intermediate nitrenium ion (Figure 1), the chlorine substitution pathway represents  $47 \pm 4\%$  of the total GSH conjugation in presence of hGST P1-1. GSH conjugate CG-5, which was tentatively assigned to the conjugate in which the GSH moiety is attached to the non-chlorinated aromatic ring, represents on average  $25 \pm 3\%$  of the GSH conjugate. Conjugate CG-1, which is the major conjugate formed in non-enzymatic GSH-conjugation, represents on average to  $22 \pm 2\%$  of the GSH conjugates. GSH conjugates CG-3 and CG-4, as shown in Figure 1, represented less than 2% of the total of GSH conjugates. GSH conjugate CG-8 that

## DMD #41046

most likely results from the chlorine substitution of the nitrenium ion of N-demethylclozapine represents  $3.5 \pm 2.3\%$  of the total GSH conjugates.

The secondary GSH conjugates, CG-2 ( $MH^+$  ion at  $m/z$  618.23) and CG-8 ( $MH^+$  ion at  $m/z$  584.25) derived from N-demethylclozapine, and CG-7 ( $MH^+$  ion at  $m/z$  903.35) derived from CG-6 ( $MH^+$  ion at  $m/z$  598.27), have not been found in human studies and therefore were not further characterized.

In order to select the most appropriate CYP102A1 M11H-mutant for large scale production of GSH conjugates, it was investigated which mutant showed a combination of high overall activity and high selectivity towards the bioactivation pathway (route d in Figure 1). Figure 3 shows the ratio of total of GSH conjugates to stable metabolites for each active mutant, ranked from low to high ratio. As shown in Figure 3, for the four most active mutants, having active site amino acids Ala87, Val87, Tyr87 and Ile87, less than 35% of the total of metabolites represented GSH conjugates. For mutants containing Gln87, Phe87 and Gly87, however, approximately 80% of the metabolites found were GSH conjugates, indicating that for these mutants bioactivation to CLZ nitrenium ion (route d, Figure 1) is the major pathway of metabolism. Because the mutant containing Phe87 has the highest activity, this mutant was selected for large scale production of GSH conjugates for structural elucidation by  $^1H$ -NMR.

### **Large scale incubation and NMR identification of isolated GSH conjugates**

Figure 4 shows the preparative HPLC chromatogram, with UV-detection at 254 nm, obtained after large scale incubation of CLZ with mutant Phe87. After isolation of the individual metabolites by preparative HPLC, their purity and identity was first analyzed by analytical HPLC and LC/MS/MS method, resulting in the assignment of metabolites and parent compound as presented in Figure 4. By hourly additions of enzymes and cofactors, over 90% of CLZ was converted, according to the strong decrease in parent compound. Based on the peak areas approximately 98% of the metabolites found are GSH conjugates. This higher percentage of GSH conjugation, when compared to the analytical scale incubations, can be explained by further bioactivation of the stable metabolite C-2, producing CG-8 and CG-2. The low yield of CLZ N-oxide (C-1) might be explained by non-enzymatic reduction of the N-oxide by NADPH and GSH that was added hourly to the incubation (Pirmohamed et al., 1995).

## DMD #41046

For the five primary GSH conjugates of CLZ, having  $MH^+$  ion at  $m/z$  632.23 (CG-1, CG-3, CG-4 and CG-5) and  $MH^+$  ion at  $m/z$  598.25 (CG-6),  $^1H$  NMR spectra were recorded to identify the position of GSH conjugation. Figure 5 shows the signals of the aromatic hydrogen atoms of the CLZ-moiety of these GSH conjugates. The COSY-spectra of these signals, which were recorded to facilitate the assignment of the aromatic hydrogen atoms as shown in Table 2, can be found as Supplementary material. The signals of the aliphatic hydrogen atoms were consistent with the glutathionyl moiety (data not shown).

Figure 5A shows the  $^1H$ -NMR spectrum of conjugate CG-1, which is the major GSH conjugate formed in absence of glutathione S-transferases (Damsten et al., 2008; Dragovic et al., 2010). This conjugate, which eluted after 32.5 min in the preparative HPLC (Figure 4), was previously identified as C-6 glutathionyl clozapine. The spectrum shown in Figure 5A is in full agreement with the  $^1H$ -NMR spectra of C-6 glutathionyl clozapine which was identified previously as the major GSH conjugate formed by peroxidases and electrochemical oxidation of CLZ (Fischer et al., 1991; Liu et al., 1995; Madsen et al., 2007). Two doublets at 6.96 and 7.23 ppm correspond to the protons at positions 9 and 7, with a small coupling constant of 2.5 Hz due to proton in the *meta*-position. Fischer et al., previously assigned doublet at 6.96 ppm to  $H_7$  and the signal at 7.23 ppm to  $H_9$  (Fischer et al., 1991). Madsen et al., however, assigned doublet at 6.96 ppm to  $H_9$  and the signal at 7.23 ppm to  $H_7$  (Madsen et al., 2007). Which signal corresponds to which proton could not be determined unequivocally, based on chemical shift and coupling pattern only (Liu et al., 1995). This, however, does not affect the identification of position of GSH conjugation because each theoretically possible GSH conjugate is expected to have its unique combination of multiplicity and coupling pattern. Therefore for signals that could not be assigned unequivocally to specific aromatic protons, two possibilities are shown in Table 2. The assignments before the slashes correspond to the first possibility, whereas the assignments after the slashes correspond to the second possibility, according to the COSY-spectra (Supplemental Figure 1).

Figure 5B shows the  $^1H$ -NMR spectrum of purified CG-3, which eluted at 32.2 min with preparative HPLC. This conjugate was previously found to be a minor GSH conjugate, with  $MH^+$  ion at  $m/z$  of 632.2, in incubations of CLZ with liver microsomes and CYP102A1 M11H when incubated in absence of glutathione S-transferases (Damsten et al., 2008; Dragovic et al. 2010). The spectrum shown in the Figure 5B can only be explained by conjugation of GSH at the C-9 position of clozapine. Two signals at 6.83 and 7.02 ppm

## DMD #41046

showed only a coupling of 8 Hz and are therefore assigned to the neighboring H<sub>6</sub> and H<sub>7</sub> protons. The COSY-spectrum of conjugate CG-3 (Supplemental Figure 2) was identical to that of C-9-glutathionyl clozapine as published previously (Liu et al., 1995). The corresponding chemical shifts and coupling constants for the observed signals are given in Table 2.

Two more conjugates having a MH<sup>+</sup> ion at m/z 632.2 eluted at retention times 30.9 min and 33.1 min (Figure 4) and appeared to correspond to conjugates CG-4 and CG-5 (Dragovic et al., 2010). Based on the order of elution and small differences in fragmentation patterns in LC/MS/MS (Maggs et al., 1995), the structure of these GSH conjugates were previously tentatively assigned to C-7 glutathionyl clozapine (CG-4) and a conjugate with GSH bound to the non-chlorinated ring (CG-5). However, so far no <sup>1</sup>H NMR spectra have been reported confirming the exact positions. Spectra for this two conjugates are shown in the Figure 5C and 5E, respectively.

Figure 5E shows the <sup>1</sup>H-NMR-spectrum of the aromatic region of CG-5, which is found at high levels when GSH conjugation is catalyzed by GST P1-1 (Figure 4). This spectrum can only be explained by conjugation of GSH at position 2 or 3 of the non-chlorinated aromatic ring. In each conjugate in which the non-chlorinated aromatic ring is not substituted, two triplets are found corresponding the protons H<sub>2</sub> and H<sub>3</sub> that are both strongly coupled by two ortho-protons, Figure 5A-D. These typical triplets could not be found in the spectrum of CG-5 (Figure 5E), indicating that one of these protons is substituted. Furthermore, the signals at 6.96, 7.37 and 7.45 ppm could be attributed to protons H<sub>6</sub>, H<sub>9</sub> and H<sub>7</sub> of the chlorinated ring, according to the COSY-spectrum (Supplemental Figure 4). This confirms that addition of the GSH is at the non-chlorinated aromatic ring. Although the loss of characteristic triplets show that GSH is conjugated to position 2 or 3, the <sup>1</sup>H-NMR and COSY-spectra could not differentiate between positions 2 or 3 for GSH binding. When GSH is bound at the 2 position, the signal at 6.85 ppm will correspond to proton H<sub>3</sub>, because this signal has a *ortho*-coupling of 8.5 Hz due to H<sub>4</sub> and a weak coupling of 1.5 Hz due to the *meta* proton in position 1. The doublet with ortho-coupling of 8.5 Hz at 6.78 ppm corresponds to H<sub>4</sub>, coupled by H<sub>3</sub>, whereas the doublet with weak coupling of 1.5 Hz at 6.95 ppm would correspond to H<sub>1</sub> by meta-coupling by proton H<sub>3</sub>. When GSH is bound at the 3-position, the signal at 6.85 ppm will correspond to proton H<sub>2</sub>, because with *ortho*-coupling of 8.5 Hz due to H<sub>1</sub> and a weak coupling of 1.5 Hz due to the *meta* proton in position 4. The doublet with ortho-coupling of 8.5 Hz at

## DMD #41046

6.78 ppm corresponds to H<sub>1</sub>, coupled by H<sub>2</sub>, whereas the doublet with weak coupling of 1.5 Hz at 6.95 ppm corresponds to H<sub>4</sub> by meta-coupling by proton H<sub>2</sub>.

Conjugate CG-4 is the fourth GSH conjugate with MH<sup>+</sup> ion at m/z 632.2, and was previously tentatively assigned to C-7 glutathionyl clozapine (Dragovic et al., 2010). However, theoretically this also can represent a conjugate with GSH bound to one of the other positions of the non-chlorinated aromatic ring. This GSH conjugate eluted at 30.9 min with preparative HPLC, Figure 4. Because this conjugate is produced at very low yield, several large scale incubations were performed to obtain enough material to record a <sup>1</sup>H-NMR-spectrum with sufficient signal-to-noise ratio. Although this small amount of the conjugate appeared to be contaminated by an unknown compound, the COSY-spectrum allowed us to solve the spectrum, despite the strong contaminant signal at 7.10 ppm, Figure 5C and supplemental Figure S3. Based on these spectra this GSH conjugate is identified as C-7 glutathionyl clozapine, consistent with the previous proposals (Maggs et al., 1995; Dragovic et al., 2010). Firstly, two triplets at 7.04 and 7.37 could be assigned to the protons H<sub>2</sub> and H<sub>3</sub>. Two sharp singlets at 7.01 and 7.03 ppm are attributed to isolated protons that do not have ortho- or meta-coupling. If GSH was bound to position 7, protons at position 6 and 9 would lose their ortho and meta couplings by H<sub>7</sub>. Two signals centered at 7.28 and 7.07 ppm represent proton H<sub>1</sub> and H<sub>4</sub>, which showed both *ortho*- and *meta*-coupling by H<sub>2</sub> and H<sub>3</sub>, Table 2. Although the signal at 7.07 partially overlaps with the signal of the impurity, the COSY-spectrum confirmed that signal centered at 7.07 ppm is a doublet with *ortho*-coupling.

The fifth GSH-conjugate for which a <sup>1</sup>H-NMR spectrum is recorded is CG-6, which was the major GSH conjugate found in the incubations in presence of hGST P1-1, and which showed a MH<sup>+</sup> ion at m/z 598.25 by LC/MS/MS-analysis. In the preparative HPLC-system used, this GSH conjugate eluted at 27.6 min, Figure 4. Figure 5D and supplemental Figure S5 show the <sup>1</sup>H-NMR and COSY-spectra obtained. Two triplets centered at 7.04 and 7.35 ppm with small *meta*-couplings correspond to the protons H<sub>3</sub> and H<sub>2</sub> at the non-chlorinated aromatic ring. The signals centered at 7.00 and 7.30 ppm correspond to protons H<sub>1</sub> and H<sub>4</sub>, as demonstrated by the combination of both *ortho* and *meta* coupling by protons H<sub>2</sub> and H<sub>3</sub>. The signals at 6.82, 7.01 and 7.12 ppm correspond to protons H<sub>6</sub>, H<sub>7</sub> and H<sub>9</sub> respectively, based on the coupling patterns and COSY-spectrum. On the basis of this spectrum and mass spectrum it was confirmed that this conjugate correspond to C-8 glutathionyl deschloroclozapine.



## Discussion

Currently, there is an increasing interest in developing novel methodologies to produce human relevant drug metabolites at large scale in order to enable structural characterization of metabolites and testing their pharmacological and toxicological properties. One of the approaches is to make use of genetically engineered cytochromes P450s that are developed for the catalysis of regio- and stereoselective hydroxylation of chemicals at high activity. In particular the bacterial cytochrome P450 CYP102A1 from *Bacillus megaterium* has high potential as a biocatalyst for these purposes, because this enzyme is the most active P450 discovered so far, and because the substrate selectivity and metabolic profile can be manipulated by site-directed and/or random mutagenesis (Yun et al., 2007; Sawayama et al., 2009). One of the CYP102A1-mutants which show high activity in drug metabolism is CYP102A1 M11H, which contains 10 different amino acid substitutions compared to wild-type CYP102A1. This CYP102A1-mutant was shown to be highly active in metabolizing a variety of drugs to human relevant metabolites, including reactive intermediates (van Vugt-Lussenburg et al. 2007; Damsten et al. 2008; Dragovic et al. 2010). Recently, we have performed a saturation mutagenesis study in which the active-site residue at position 87 was mutated to all 20 possible amino acids (Vottero et al., 2011). In CYP102A1 M11H the residue at this position is Val87, which was introduced at an early stage of the mutagenesis process, to expand the substrate selectivity to drug metabolism (Lussenburg et al., 2005). In the saturation mutagenesis study in which all amino acids were evaluated at position 87, we recently demonstrated that the type of amino acid at position 87 has strong effect on substrate selectivity when comparing a series of alkoxyresorufins (Vottero et al., 2011). In this study it was also demonstrated that the nature of the amino acid at position 87, strongly influences the regioselectivity of testosterone hydroxylation of CYP102A1 M11H.

In the present study, the library of CYP102A1 M11H-mutants with different amino acids at position 87 was evaluated with CLZ as substrate. CLZ is a drug that can be metabolized by peroxidases and P450s to multiple metabolites, including reactive nitrenium ions that might be involved in adverse drug reactions associated with CLZ therapy. CYP102A1 M11H has been shown to produce high levels of most human relevant metabolites of CLZ, which are represented in Figure 1. All metabolites can be explained by four different initial oxidative pathways: N-demethylation (a), N-oxidation (b), piperazine-ring opening (c) and dehydrogenation to a reactive nitrenium ion (d). Although CYP102A1 M11H with residue

## DMD #41046

Val87 produced significant amounts of reactive nitrenium ion (as identified as GSH conjugates), the major pathways of metabolism are N-demethylation and N-oxidation, which explain approximately 70% of the total of metabolites. The aim of this study was to investigate whether residue 87 also controls regioselectivity of CLZ metabolism, and to investigate whether a mutant could be identified with higher selectivity toward the bioactivation to the toxicologically relevant CLZ nitrenium ion. A more selective P450 CYP102A1 mutant would be more useful for the generation of high levels of CLZ GSH-conjugates that still require structural confirmation by  $^1\text{H-NMR}$ . So far, the structure of only two of the GSH-conjugates shown in Figure 1 has been elucidated by  $^1\text{H-NMR}$  and mass spectrometry. However, the structures of the GSH-conjugates found in bile of rats and mice, and which also have  $\text{MH}^+$  ions at  $m/z$  632.2 (Maggs et al., 1995) have not yet been characterized by  $^1\text{H-NMR}$ .

As shown in Table 1, changing the amino acid residue at position 87 of CYP102A1 M11H has strong effects on both total activity and regioselectivity of CLZ oxidation. The mutants Ala87, Val87, and Ile87 were found to be the most active, as was found previously with alkoxyresorufins and testosterone (Vottero et al., 2011). These mutants have a small and apolar residue in position 87. This seems consistent with the previous hypothesis that replacement of the bulky Phe87 in wild type CYP102A1 by smaller amino acids creates space for the bulky substrates which allows better positioning with respect to the activated oxygen species, resulting in higher activities and coupling efficiencies (Carmichael and Wong, 2001; Landwehr et al., 2006; Li et al., 2001). However, in the present study relatively high activities were also found in the CYP102A1 M11H mutants containing the relatively bulky amino acids Phe87, Tyr87 and Trp87. Previously, replacing Phe87 by Tyr87 in wild-type CYP102A1 was found to be detrimental for activity towards long-chain fatty acids, probably by disruption of the hydrophobic interaction by the phenol-group. In case of CYP102A1 M11H the presence of these bulky amino acids apparently is less restrictive for bulky substrates because in presence of Phe87 and Tyr87 both testosterone (Vottero et al., 2011) and CLZ are metabolized at high activity. Apparently, by the combination of ten mutations present in CYP102A1 M11H the topology of the active site and/or substrate access channel has changed significantly, explaining the much wider substrate selectivity compared to wild-type CYP102A1.

As shown in Figure 2A, the nature of amino acid 87 has strong effect on regioselectivity of CLZ metabolism. When considering the stable metabolites that are formed

## DMD #41046

via pathways a, b and c (Figure 1), the major metabolite with all mutants was N-demethylclozapine (C-2), although the N-oxide (C-1) was also produced at significant levels. However, the ratio of N-demethylation to N-oxidation appeared to be quite dependent on the nature of amino acid residue at position 87. For example, for the mutants containing Leu87 and Ile87, N-demethylation was almost 10-fold higher than N-oxidation. In the mutant containing Phe87, N-demethylclozapine and CLZ N-oxide were formed in almost the same amount. However, the relative contribution of N-oxidation in all incubations might be somewhat underestimated, because all incubations were performed in presence of GSH that is known to reduce CLZ N-oxide back to CLZ (Tugnait et al., 1999). Therefore, in case of Phe87 N-oxidation of CLZ might even be higher in absence of reductive agents. In case of the human P450s, it has been shown that CYP1A2 preferentially metabolizes CLZ by N-demethylation, whereas CYP3A4 is mainly responsible for production of CLZ N-oxide (Tugnait et al., 1999). What factors determine the ratio of N-demethylation and N-oxidation is still unclear, however. Different presentation of the piperazine N-methyl group to the oxidative species at the active site might explain why some human P450s preferentially catalyze N-demethylation, whereas others predominantly catalyze N-oxidation.

One of the aims of the present study was to identify mutants with high activity and selectivity for bioactivation of CLZ to the reactive nitrenium ion. As shown in Figure 2A several mutants produced high levels of GSH conjugates (CG-total), indicative for relative high selectivity in the formation of the reactive nitrenium ion. Other mutants showed strong preference in catalyzing formation of N-demethylclozapine and CLZ N-oxide. However, from the results it is unclear what features of the amino acid side-chain determines selectivity for bioactivation. For example, the CYP102A1 M11H-mutant containing the bulky Phe87 showed high selectivity and activity in formation of GSH conjugates, whereas the mutants containing the bulky Tyr87 and Trp87 preferentially catalyzed formation of stable metabolites. Future detailed protein modeling studies including those evaluating protein dynamics and substrate mobility might help to rationalize the different regioselectivities observed. Figure 2B shows the relative amounts of the different GSH conjugates that are formed in incubations of CLZ with CYP102A1 mutants in presence of recombinant hGST P1-1. Consistent with our previous study, the major pathway of GST P1-1 catalysed GSH conjugation is substitution of the chlorine-atom of the CLZ nitrenium ion (Dragovic et al., 2010). The resulting GSH bound nitrenium ion is subsequently reduced by NADPH or GSH, to form CG-6, or further

## DMD #41046

conjugated to GSH, to form CG-7 (Figure 1). The fact that with all mutants the same ratio of GSH conjugates is formed strongly suggests that all form from the same reactive intermediate.

Mutant Phe87 was selected for large scale biosynthesis of GSH conjugates because this mutant combined high activity with high preference for the bioactivation pathway, Figure 3. Previous studies, aiming at the characterization of GSH conjugates of CLZ, showed that non-enzymatic GSH conjugation to the CLZ nitrenium ion, formed by peroxidases or electrochemically, mainly produced a GSH conjugate bound at the C-6 position of CLZ and minor amounts of conjugate bound at the C-9 position. The structures of these two GSH conjugates have been elucidated by  $^1\text{H-NMR}$ . However, *in vivo* studies with rats and mice have shown that in bile two major GSH conjugates are excreted that do not correspond to these two conjugates (Maggs et al., 1995). Also, incubations with rat liver microsomes showed small amounts of a fifth GSH conjugate with  $\text{MH}^+$  ion at  $m/z$  632.2 (Maggs et al., 1995). It was initially concluded that these GSH conjugates might originate from as yet unidentified reactive intermediate produced *in vivo*. However, we recently demonstrated that these alternative GSH conjugates probably are resulting from GST catalyzed inactivation of the CLZ nitrenium ion (Dragovic et al., 2010). By using mutant Phe87, we were able to produce significant amounts of all GSH conjugates, for which the structures were not yet elucidated unequivocally by  $^1\text{H-NMR}$ . Because four GSH conjugates were found with  $\text{MH}^+$  ion at  $m/z$  632.2, it was previously concluded that for at least one of the conjugates, GSH is bound to the non-chlorinated aromatic ring of CLZ. The present study shows that conjugate designed CG-5, which is a major product in presence of hGST P1-1 has the GSH moiety bound to the non-chlorinated ring at the position 2 or 3 (Figure 5). For the minor conjugates CG-4, we were able to confirm binding at the 7 position, as it was tentatively assigned based on fragmentation pattern in LC/MS/MS (Maggs et al., 1995).

In conclusion, the present study shows that mutation of residue 87 in drug metabolizing mutant CYP102A1 M11H has strong influence on activity and regioselectivity of CLZ metabolism. Using a mutant that combined high activity and high selectivity for CLZ bioactivation, we were able to produce sufficient amounts of as yet tentatively assigned GSH conjugates to characterize their structures by  $^1\text{H-NMR}$ . This study confirms the high potential of CYP102A1-mutants as tool to characterize human-relevant metabolites.

DMD #41046

## Authorship Contributions

*Participated in research design:* Rea, Dragovic, Vermeulen, Commandeur

*Conducted experiments:* Rea, Dragovic, Boerma, De Kanter

*Contributed new reagents and analytical tools:* Boerma

*Performed data analysis:* Rea, Dragovic, De Kanter, Commandeur

*Wrote or contributed to the writing of the manuscript:* Rea, Dragovic, Commandeur

## References

- Bradford M (1976) A rapid and sensitive method for the quantitation of microgram quantities of protein utilizing the principle of protein-dye binding. *Anal Biochem* **72**: 248-254.
- Buchanan RW (1995) Clozapine: efficacy and safety. *Schizophrenia bull* **21**:579-591.
- Carmichael AB and Wong LL (2001) Protein engineering of *Bacillus megaterium* CYP102A1 — the oxidation of polycyclic aromatic hydrocarbons. *Eur J Biochem* **268**: 3117-3125.
- Damsten MC, Van Vugt-Lussenburg BM, Zeldenthuis T, De Vlieger JS, Commandeur JNM, and Vermeulen NPE (2008) Application of drug metabolizing mutants of cytochrome P450 BM3 (CYP102A1) as biocatalysts for the generation of reactive metabolites. *Chem Biol Interact* **171**: 96-107.
- Dragovic S, Boerma JS, van Bergen L, Vermeulen NPE, and Commandeur JNM (2010) Role of human glutathione S-transferases in the inactivation of reactive metabolites of clozapine. *Chem Res Toxicol* **23**:1467-1476.
- Evans WE and Relling MV (1999) Pharmacogenomics: translating functional genomics into rational therapeutics, *Science* **286**: 487–491.
- Fischer V, Haar JA, Greiner L, Lloyd RV, and Mason RP (1991) Possible role of free radical formation in clozapine (Clorazil) induced agranulocytosis. *Mol Pharmacol* **40**: 846-853.
- Habig WH, Pabst MJ, and Jakoby BJ (1974) Glutathione S-transferases. The first enzymatic step in mercapturic acid formation. *J Biol Chem* **249**: 7130-7139.
- Hummer M, Kurz M, Kurzthaler I, Oberbauer H, Miller C, and Fleischhacker WW , (1997) Hepatotoxicity of clozapine. *J Clin Psychopharm* **17**: 314-317.
- Kim KH, Kang JY, Kim DH, Park SH, Park SH, Kim D, Park KD, Lee YJ, Jung HC, Pan JG, Ahn T, and Yun CH (2011) Generation of human chiral metabolites of simvastatin and lovastatin by bacterial CYP102A1 mutants. *Drug Metab Dispos* **39**: 140-150.
- Landwehr M, Hochrein L, Otey CR, Kasrayan A, Bäckvall JE, and Arnold FH (2006) Enantioselective  $\alpha$ -hydroxylation of 2-arylacetic acid derivatives and buspirone catalyzed by engineered cytochrome P450 BM-3. *J Am Chem Soc* **128**: 6058-6059.

DMD #41046

Li QS, Ogawa J, Schmid RD, and Shimizu S (2001) Engineering cytochrome P450 BM-3 for oxidation of polycyclic aromatic hydrocarbons. *Appl Environ Microbiol* **67**: 5735-5739.

Liu ZC and Uetrecht JP (1995) Clozapine is oxidized by activated human neutrophils to a reactive nitrenium ion that irreversibly binds to the cells. *J Pharmacol Exp Ther* **275**: 1476-1483.

Lussenburg BMA, Babel LC, Vermeulen NPE, and Commandeur JNM (2005) Evaluation of alkoxy-resorufins as fluorescent substrates for cytochrome P450 BM3 and site-directed mutants. *Anal Biochem* **341**:148-155.

Madsen KG, Olsen J, Skonberg C, Hansen SH, and Jurva U (2007) Development and evaluation of an electrochemical method for studying reactive phase-I metabolites: correlation to *in vitro* drug metabolism. *Chem Res Toxicol* **20**: 821-831.

Maggs JL, Williams D, Piromohamed M, and Park, BK (1995) The metabolic formation of reactive intermediates from clozapine, a drug associated with agranulocytosis in man, *J Pharmacol Exp Ther* **275**:1463-1475.

Ost TW, Miles CS, Murdoch J, Cheung Y, Reid GA, Chapman SK, and Munro AW (2000) Rational re-design of the substrate binding site of flavocytochrome P450 BM3. *FEBS Lett* **486**: 173-177.

Pirmohamed M, Williams D, Madden S, Templeton, E, and Park BK (1995) Metabolism and bioactivation of clozapine by human liver *in vitro*. *J Pharmacol Exp Ther* **272**: 984-990.

Safferman A, Lieberman JA, Kane JM, Szymanski S, and Kinon B (1991) Update on the clinical efficacy and side effects of clozapine. *Schizophrenia bulletin* **17**: 247-261.

Sawayama AM, Chen MM, Kulanthaivel P, Kuo MS, Hemmerle H, and Arnold FH (2009) A panel of cytochrome P450 BM3 variants to produce drug metabolites and diversify lead compounds. *Chemistry* **15**: 11723-11729.

Shimada T, Yamazaki H, Mimura M, Inui Y, and Guengerich FP (1994) Interindividual variations in human liver cytochrome P-450 enzymes involved in the oxidation of drugs, carcinogens and toxic chemicals: studies with liver microsomes of 30 Japanese and 30 Caucasians, *J Pharmacol Exp Ther* **270**: 414-423.

DMD #41046

Smith, D.A., and Obach, R.S. (2009) Metabolites in safety testing (MIST): considerations of mechanisms of toxicity with dose, abundance, and duration of treatment. *Chem.Res.Toxicol.* **22**: 267-279.

Tugnait, M., Hawes, E.M., McKay, G., Eichelbaum, M. and Midha, K.K. (1999) Characterization of the human hepatic cytochromes P450 involved in the in vitro oxidation of clozapine. *Chem.-Biol.Interact.* **118**: , 171-189.

Van Vugt-Lussenburg BM, Stjerschantz E, Lastdrager J, Oostenbrink C, Vermeulen NP, and Commandeur JN (2007) Identification of critical residues in novel drug metabolizing mutants of cytochrome P450 BM3 using random mutagenesis. *J Med Chem* **50**: 455-461.

Vottero E, Rea V, Lastdrager J, Vermeulen NPE, and Commandeur JNM (2011) Effect of residue 87 on the substrate and regioselectivity of drug metabolizing cytochrome P450 BM3 mutant M11, *J.Biol.Inorg.Chem.* (2011) PMID: 21567268.

Wagstaff AJ, and Perry CM (2003) Clozapine in prevention of suicide in patients with schizophrenia or schizoaffective disorder. *CNS Drugs* **17**: 273-280.

Yun CH, Kim KH, Kim DH, Jung HC, and Pan JG (2007) The bacterial P450 BM3: A prototype for a biocatalyst with human P450 activities. *Trends Biotechnol* **25**: 289-298.



## **Footnotes:**

Vanina Rea and Sanja Dragovic contributed equally to this work.

This research was performed within the framework of projects D2-102 (VR) and D3-201 (SD and JSB) of the Dutch Top Institute Pharma.

## Legends to the Figures

### Figure 1.

Oxidative pathways of metabolism of CLZ by cytochrome P450 and non-enzymatic and enzymatic conjugation reactions of reactive CLZ nitrenium ion by glutathione (GSH) and glutathione S-transferase (GST): a) N-demethylation; b) N-oxidation; c) oxidative opening of piperazine-ring; d) dehydrogenation to nitrenium ion.

### Figure 2.

Relative amounts of CLZ metabolites formed by CYP102A1 M11H mutants with different amino acid residues at position 87. Incubations were carried out for 30 minutes in presence of 100  $\mu$ M GSH and 8  $\mu$ M recombinant human GST P1-1. (A) relative amounts of stable CLZ-metabolites (C-1 to C-5) and total of GSH-conjugates (CG-total); (B) relative amounts of individual GSH-conjugates.

### Figure 3.

Percentage of total of GSH-conjugates formed in incubations of CLZ with CYP102A1 M11H mutants with different amino acid residues at position 87, ranked in order of activity. *Numbers below each bar* represent the activity of the CYP102A1 M11H mutants relative to the most active mutant CYP102A1 M11H Ala87.

### Figure 4.

Preparative HPLC-UV chromatogram of metabolites obtained by large scale incubation of CLZ with CYP102A1 M11H Phe87 in presence of hGST P1-1 and GSH.

### Figure 5.

Aromatic regions of the  $^1\text{H-NMR}$  spectra of clozapine GSH-conjugates. The conjugates were obtained by purification by preparative HPLC of metabolites formed by CYP102A1 M11H Phe87, GSH and hGSTP1-1. (A) CG-1, C-6 glutathionyl CLZ; (B) CG-3, C-9 glutathionyl CLZ; (C) CG-4, C-7 glutathionyl CLZ; (D) CG-6, C-8 glutathionyl deschloroclozapine; (E) CG-5, C-2 glutathionyl CLZ or C-3 glutathionyl CLZ.

## DMD #41046

**Table 1.** Effect of aminoacid at position 87 in CYP102A1 M11H on the GSH-conjugation to reactive metabolites formed by oxidative bioactivation of clozapine.

m/z (MH <sup>+</sup> )	C-1 343	C-2 313	C-3 301	C-4 287	C-5 329	CG-1 632	CG-2 618	CG-3 632	CG-4 632	CG-5 632	CG-6 598	CG-7 903	CG-8 584	Specific activity*)	% conversion
<i>Apolar side chain</i>															
Gly87	0.4	0.7	0.1	0.0	0.0	1.1	0.0	0.1	0.0	1.2	2.7	0.5	0.4	1.2	1.4
Ala87	35.1	82.5	1.1	2.0	7.8	13.7	0.7	1.0	0.3	14.4	26.1	4.0	2.5	31.9	38.2
Val87	15.1	90.1	0.9	1.0	7.1	9.3	0.7	0.8	0.3	11.7	15.8	5.5	2.9	26.9	32.3
Leu87	1.0	9.0	0.3	0.1	0.0	3.2	0.1	0.5	0.3	4.7	6.3	1.2	0.6	4.6	5.5
Ile87	6.8	71.4	0.5	0.3	0.6	9.6	0.5	0.8	0.4	0.0	20.7	2.9	1.6	21.6	25.9
Phe87	8.7	10.5	0.2	0.2	0.0	18.2	0.2	0.9	0.3	16.7	37.2	5.3	2.2	16.8	20.1
Trp87	11.6	46.9	0.0	0.0	0.0	5.0	0.0	0.0	0.0	5.4	7.6	2.7	0.8	13.3	16.0
Met87	0.7	5.5	0.1	0.1	0.0	2.8	0.0	0.3	0.0	3.5	5.1	0.0	0.7	3.2	3.8
Pro87	1.4	4.6	0.0	0.0	0.0	0.0	0.0	0.0	0.0	0.0	0.0	0.0	0.0	n.d. **)	1.2
<i>Polar uncharged side chain</i>															
Tyr87	16.5	73.4	0.9	0.9	5.2	6.7	0.3	0.5	0.2	8.1	11.5	3.0	1.1	21.4	25.7
Gln87	3.2	6.4	0.1	0.1	0.0	8.5	0.1	0.7	0.3	9.7	13.9	1.9	2.1	7.9	9.4
Asn87	0.7	3.2	0.2	0.2	0.0	2.3	0.0	0.2	0.0	2.8	4.7	1.0	0.7	2.6	3.2
Cys87	0.2	1.0	0.3	0.0	0.0	1.0	0.0	0.0	0.0	1.0	2.0	0.0	0.0	0.9	1.1
Ser87	n.d.	n.d.	n.d.	n.d.	n.d.	n.d.	n.d.	n.d.	n.d.	n.d.	n.d.	n.d.	n.d.	n.d.	n.d.
Thr87	n.d.	n.d.	n.d.	n.d.	n.d.	n.d.	n.d.	n.d.	n.d.	n.d.	n.d.	n.d.	n.d.	n.d.	n.d.
<i>Polar charged side chain</i>															
Asp87	8.5	13.6	0.0	0.0	0.0	3.7	0.0	0.0	0.0	3.7	7.1	0.3	0.3	n.d. **) 7.4	
Glu87	0.6	4.3	0.1	0.1	0.0	1.7	0.0	0.0	0.0	1.7	3.1	0.5	0.0	2.0	2.4
His87	0.9	1.3	0.3	0.1	0.0	0.9	0.0	0.0	0.0	1.1	1.6	0.0	0.0	1.0	1.2
Arg87	1.7	4.5	0.0	0.0	0.0	0.0	0.0	0.0	0.0	0.0	0.0	0.0	0.0	1.0	1.2

Concentration of metabolites ( $\mu\text{M}$ ) formed after 30 minutes incubations of 200 nM CYP102A1 with 500  $\mu\text{M}$  clozapine, 8  $\mu\text{M}$  GST P1-1 in presence of 100  $\mu\text{M}$  GSH. Values represent averages of three individual experiments; standard errors were always lower than 10%.

\*(nmol product/nmol CYP102A1/30min),;

\*\* P450 concentration could not be quantified (CO difference spectrum only showed a peak at 420 nm).

**Table 2.** LC-MS/MS characteristics and  $^1\text{H}$  NMR spectra of the aromatic hydrogen atoms of the GSH conjugates of clozapine

Conjugate	1H-NMR-spectra			LC-MS/MS- mass spectra m/z (intensity) <sup>b)</sup>
	Assignment <sup>a)</sup>	$\delta$ ppm (intensity)	multiplicity: coupling constants	
CG-1	H <sub>1</sub> /H <sub>4</sub>	7.30 (1H)	d of d: $^2J_{\text{HH}}$ , 7 Hz; $^3J_{\text{HH}}$ , 1.5 Hz	623.23 (MH <sup>+</sup> ; 100%); 614.22 (8%); 575.17 (6%); 503.18 (37%); 446.12 (1%); 359.12 (29 %); 302.06 (12%)
	H <sub>2</sub> /H <sub>3</sub>	7.08 (1H)	d of t: $^2J_{\text{HH}}$ 7.5 Hz, $^3J_{\text{HH}}$ 1.5 Hz	
	H <sub>3</sub> /H <sub>2</sub>	7.41 (1H)	d of t: $^2J_{\text{HH}}$ 7.5 Hz, $^3J_{\text{HH}}$ 1.5 Hz	
	H <sub>4</sub> /H <sub>1</sub>	7.10 (1H)	d: $^2J_{\text{HH}}$ 7.5 Hz	
	H <sub>7</sub> /H <sub>9</sub>	7.23 (1H)	d: $^2J_{\text{HH}}$ 2.5 Hz	
	H <sub>9</sub> /H <sub>7</sub>	6.96 (1H)	d: $^2J_{\text{HH}}$ 2.5 Hz	
CG-3	H <sub>1</sub> /H <sub>4</sub>	7.36 (1H)	d: $^2J_{\text{HH}}$ 8 Hz	623.23 (MH <sup>+</sup> ; 100%); 614.22 (1%); 503.18 (23%); 446.12 (1%); 359.12 (41%); 302.06 (6%)
	H <sub>2</sub> /H <sub>3</sub>	7.07 (1H)	d of t: $^2J_{\text{HH}}$ 7 Hz, $^3J_{\text{HH}}$ 1.5 Hz	
	H <sub>3</sub> /H <sub>2</sub>	7.37 (1H)	t: $^2J_{\text{HH}}$ 7 Hz	
	H <sub>4</sub> /H <sub>1</sub>	6.99 (1H)	d: $^2J_{\text{HH}}$ 8 Hz	
	H <sub>6</sub>	7.02 (1H)	d: $^2J_{\text{HH}}$ 8 Hz	
	H <sub>7</sub>	6.83 (1H)	d: $^2J_{\text{HH}}$ 8 Hz	
CG-4	H <sub>1</sub> /H <sub>4</sub>	7.28 (1H)	d of d: $^2J_{\text{HH}}$ 8 Hz, $^3J_{\text{HH}}$ 1.5 Hz	623.23 (MH <sup>+</sup> ; 100%); 614.22 (8%); 575.17 (3%); 503.18 (44%); 446.12 (4%); 359.12 (17 %); 302.06 (4%); 243.06 (5%)
	H <sub>2</sub> /H <sub>3</sub>	7.04 (1H)	t: $^2J_{\text{HH}}$ 7 Hz	
	H <sub>3</sub> /H <sub>2</sub>	7.37 (1H)	d of t: $^2J_{\text{HH}}$ 7 Hz, $^3J_{\text{HH}}$ 1.5 Hz	
	H <sub>4</sub> /H <sub>1</sub>	7.07 (1H)	d: $^2J_{\text{HH}}$ 8 Hz	
	H <sub>6</sub> /H <sub>9</sub>	7.01 (1H)	s	
	H <sub>9</sub> /H <sub>6</sub>	7.03 (1H)	s	
CG-5	H <sub>1</sub> /H <sub>4</sub>	6.95 (1H)	d: $^3J_{\text{HH}}$ 1 Hz	623.23 (MH <sup>+</sup> ; 100%); 614.22 (6%); 575.17 (10%); 503.18 (27%); 446.12 (25%); 359.12 (15 %); 302.06 (13%); 243.06 (34%)
	H <sub>3</sub> or H <sub>2</sub>	6.85 (1H)	d of d: $^2J_{\text{HH}}$ 8.5 Hz, $^3J_{\text{HH}}$ 2 Hz	
	H <sub>4</sub> /H <sub>1</sub>	6.78 (1H)	d: $^2J_{\text{HH}}$ 9 Hz	
	H <sub>6</sub>	6.96 (1H)	d: $^2J_{\text{HH}}$ 9 Hz	
	H <sub>7</sub>	7.45 (1H)	d of d: $^2J_{\text{HH}}$ 9 Hz, $^3J_{\text{HH}}$ 2 Hz	
	H <sub>9</sub>	7.37 (1H)	d: $^2J_{\text{HH}}$ 2 Hz	

## DMD #41046

*(Table 2 continued)*

CG-6	H <sub>1</sub> /H <sub>4</sub>	7.00 (1H)	d of d: <sup>2</sup> J <sub>HH</sub> 8 Hz, <sup>3</sup> J <sub>HH</sub> 2 Hz	598.25 (MH <sup>+</sup> ; 100%);
	H <sub>2</sub> /H <sub>3</sub>	7.35 (1H)	d of t: <sup>2</sup> J <sub>HH</sub> 7.5 Hz, <sup>3</sup> J <sub>HH</sub> 1.5 Hz	580.24 (8%); 469.20 (77%);
	H <sub>3</sub> /H <sub>2</sub>	7.04 (1H)	d of t: <sup>2</sup> J <sub>HH</sub> 7.5 Hz, <sup>2</sup> J <sub>HH</sub> 1 Hz	412.20 (4%); 325.15 (24%);
	H <sub>4</sub> /H <sub>1</sub>	7.30 (1H)	d of d: <sup>2</sup> J <sub>HH</sub> 7.5 Hz, <sup>3</sup> J <sub>HH</sub> 1 Hz	268.09 (6%)
	H <sub>6</sub>	6.82 (1H)	d: <sup>2</sup> J <sub>HH</sub> 8 Hz	
	H <sub>7</sub>	7.01 (1H)	d: <sup>2</sup> J <sub>HH</sub> 8 Hz	
	H <sub>9</sub>	7.12 (1H)	d: <sup>3</sup> J <sub>HH</sub> 2 Hz	

a) Absolute assignment of protons was not possible, therefore each signal is indicated by two assignments corresponding to two possible solutions. Assignments before the slash correspond to solution 1; assignments after the slash correspond to solution 2.

b) Electrospray spectra (LC-MS/MS) were acquired using nitrogen as collision gas with collision energy of 25V.

Figure 1

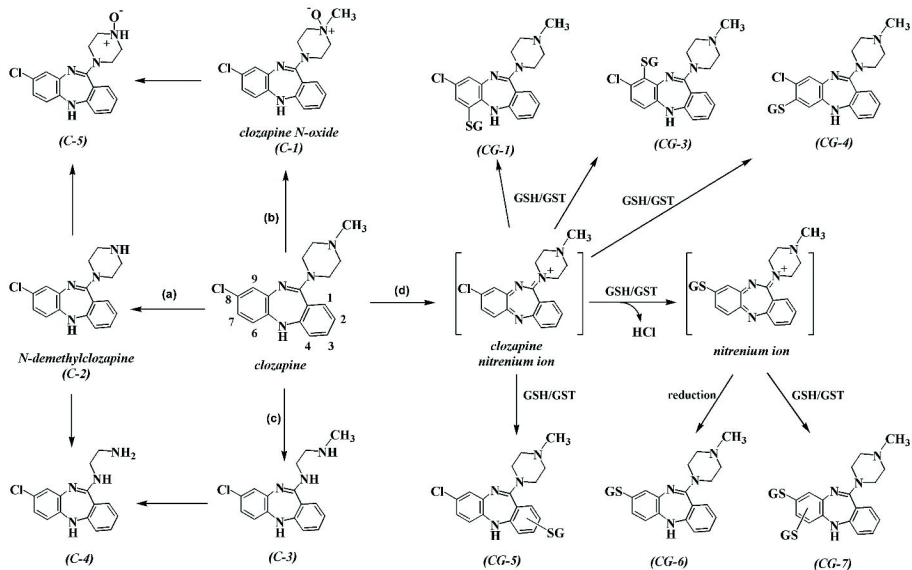


Figure 2

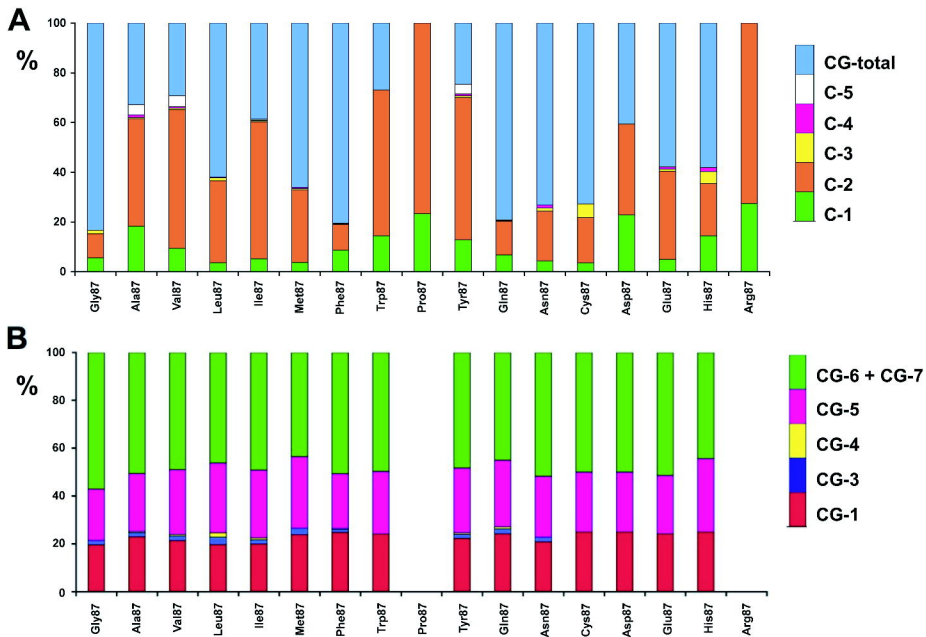


Figure 3

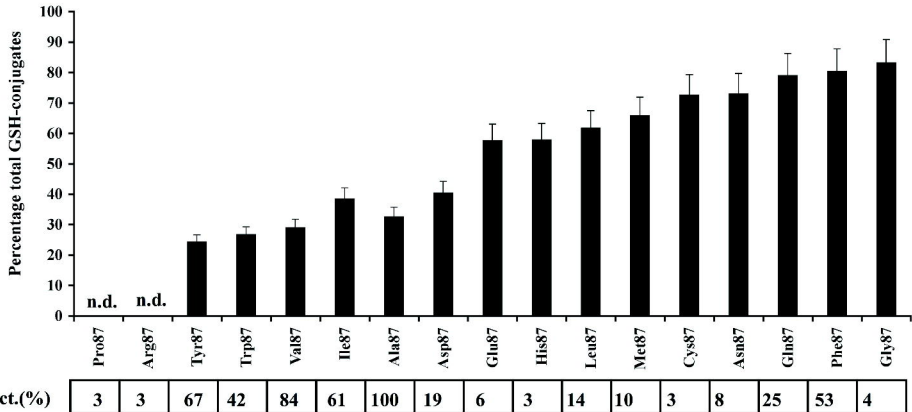




Figure 4

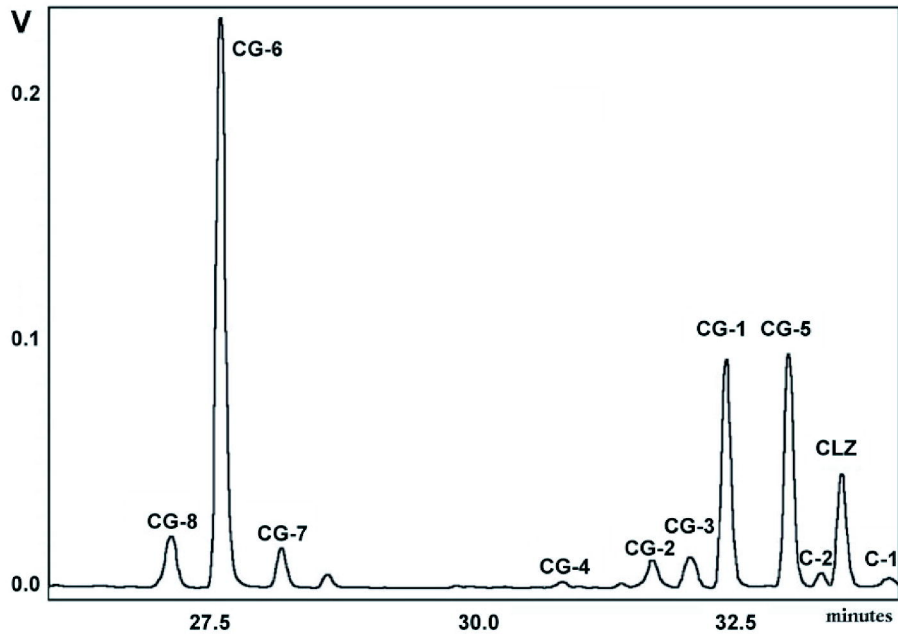


Figure 5

